ACCADEMIA NAZIONALE DEI LINCEI
Estratto dai *Rendiconti della Classe di Scienze fisiche, matematiche e naturali*
Serie VIII, vol. LV, fasc. 3-4 (Settembre-Ottobre) - Ferie 1973

Fisica delle alte energie. — *Study of photon-photon interactions by the $e^+ e^-$ Frascati storage ring.* Nota (*) di G. BARBIELLINI, F. CERADINI, S. D'ANGELO, M. GRILLI, S. ORITO, L. PAOLUZI, R. SANTONICO, T. TSURU, V. VALENTE e V. VISENTIN, presentata dal Socio M. CONVERSI.

RIASSUNTO. — La produzione di coppie di leptoni da due fotoni quasi reali è stata investigata sperimentalmente presso l'anello di accumulazione di elettroni e positroni «Adone». La tecnica usata consiste nella rivelazione dei leptoni prodotti, tramite un telescopio di contatori a scintillazione e camere a scintilla, e degli elettroni iniziali, sorgenti naturali di fotoni, tramite contatori a scintillazione che coprono gli angoli essenzialmente in avanti rispetto alla direzione del fascio. In totale sono stati registrati tredici eventi del tipo $e\bar{e} \to e\bar{e}\, e\bar{e}$, e sette eventi del tipo $e\bar{e} \to e\bar{e}\, \mu\mu^-$.

§ 1. INTRODUCTION

It has recently been shown by several Authors [1–6] that the processes $e^+ e^- \to e^+ e^- X$, where X is an $e^+ e^-$ or a $\mu^+ \mu^-$ pair, or any hadron state with $C = +1$, occur with relatively large total cross-sections already in the GeV region. This implies that the study of the collisions between the almost real photons becomes feaseble with $e^+ e^-$ storage rings for energy in excess of about 1 GeV per beam.

We stress that, in addition to the study of the higher order electromagnetic processes, these photon-photon processes provide a powerful means to survey the $C = +1$ meson resonances which couple to the two photon intermediate state. At the same time, due to their large cross-sections, these processes might give a non-negligible contamination in the course of experiments on the comparatively rare $e^+ e^-$ annihilation into hadronic final states. A clean separation between the annihilation and the photon-photon processes should be performed therefore in any case.

In an attempt to identify the photon-photon processes on an event by event basis, a tagging system has been proposed [7] to detect the forward going $e^\pm$ utilizing the machine bending magnets as momentum analizers.

We present in this report the results obtained by this tagging technique with the Frascati storage ring, Adone, for the processes $e^+ e^- \to e^+ e^- e^+ e^-$ and $e^+ e^- \to e^+ e^- \mu^+ \mu^-$, at incident energies around 800 MeV. We recall that two experimental results were recently reported on the process $e^+ e^- \to \to e^+ e^- e^+ e^-$. The experiment with VEPP II [8] was done without tagging

(*) Pervenuta all'Accademia il 19 ottobre 1973.

the forward-going $e^+ e^-$, the other experiment with Adone [9] utilized tagging counters of limited $e^\pm$ momentum acceptance (0.7 to 0.9 E, where E is the incident beam energy).

§ 2. Apparatus

Fig. 1 shows the experimental set-up. It consists of the two tagging counters (T_1 , T_r) placed inside the machine bending magnets, two photon shower counters (S_1 , S_r) set on the line of the colliding beams and two wide angle telescopes (E , I) which were employed in previous experiments by the " μ–π group " at Adone [10] [11].

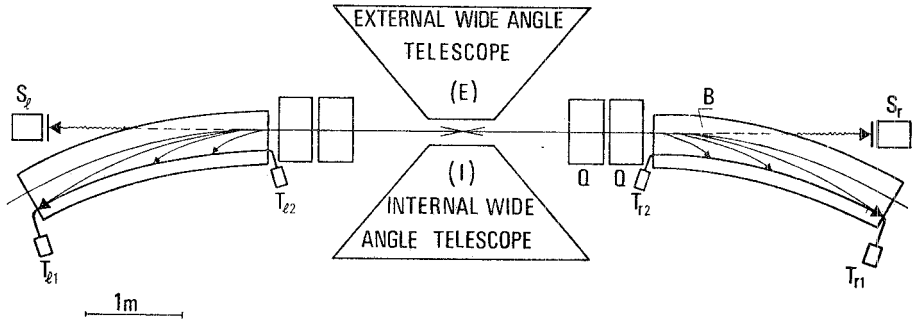

Fig. 1. – Experimental arrangement.

The tagging counters detect and measure the momenta of the forward-going $e^\pm$ which has lost the energy by irradiating the quasi real photon. The $e^\pm$ traveling essentially in the beam direction, passes through the quadrupole magnets (Q), is bent by the bending magnets (B), and is detected by the counter (T_1 , T_r). Each tagging counter is a plastic scintillator 2.45 m long, 6 cm high and 2 cm thick, viewed by two Philips 56 AVP photomultipliers (T_1 and T_2) placed on the opposite sides of the counter. The time between the signals from the two phototubes determines the impact point. From the impact point thus obtained one derives the momentum of the $e^\pm$ since a detailed map of the magnetic field is available [12]. The momentum acceptance of the tagging system is $0.1 \leq x \leq 0.8$, where $x = P/P_0$, P being the momentum of the detected $e^\pm$ and P_0 the beam momentum. A typical momentum resolution is $\Delta p/p = \pm 4\%$ (1) at $x = 0.7$, corresponding to $\Delta k/k = \pm 10\%$ for the energy of the quasi real photons ($k = E - p$).

The material just in front of the counters is represented by the wall of the vacuum chamber and in addition the thermal shielding used to protect the scintillator during the baking-up of the vacuum chamber. These amount to a perpendicular thickness of 2.7 g cm^{-2} iron equivalent, corresponding to

(1) This momentum resolution is mainly due to the finite angular spread of the surviving $e^\pm$ and to the time resolution of the phototubes. This momentum accuracy has been verified on the basis of 8 doubly tagged $e^+ e^- \to e^+ e^- \mu^+ \mu^-$ events obtained at higher energies (to be published).

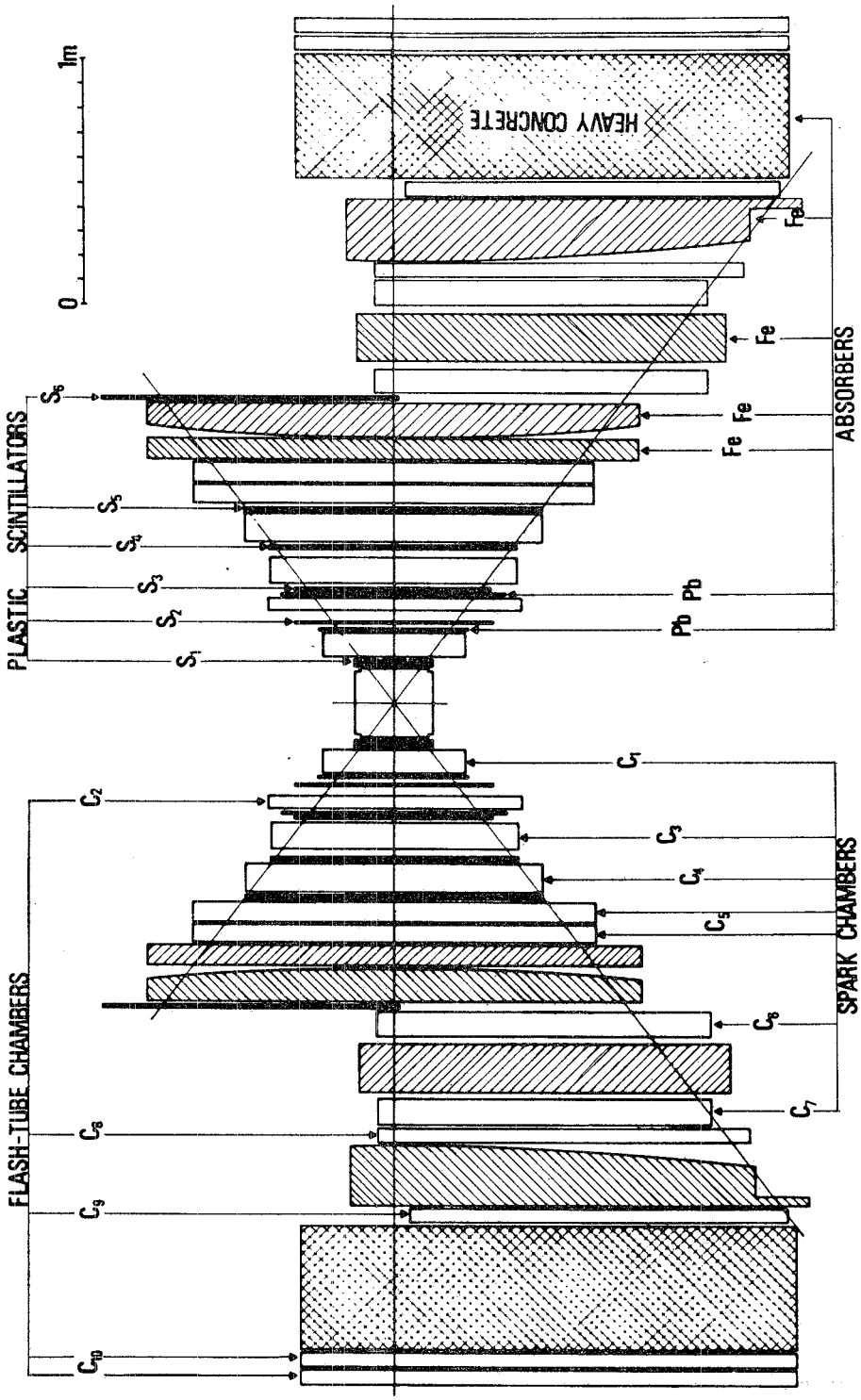

Fig. 2. – Cross-sectional view of the wide angle telescopes.

a maximum path thickness of two radiation lengths for the $e^{\pm}$ which enter with maximum inclination angles.

The photon detectors [13] S_1 and S_r are used to veto the background due to the beam gas and beam-beam bremsstrahlung, by detecting the real photons emitted at a very small angles. Each photon detector consists of an anticounter, a lead collimator and a lead-scintillator-sandwich, set at zero degree with an angular acceptance of ± 6 m rad. The measured energy resolution is $\Delta E_\gamma/E_\gamma = 0.1\ E_\gamma$, where E_γ is the photon energy expressed in GeV.

The two wide angle telescopes (E , I) reproduced in fig. 2 and described in previous papers [10] [11] are used to detect the final particles produced by the collision of the quasi real photons. They are counter and optical spark chamber telescopes each with angular acceptance of $\Delta\vartheta = \pm 45°$, $\Delta\varphi = 0.2 \times 2\pi$, giving a combined solid angle of 25 % for a point source at the center of the $e^+ e^-$ collisions region. The plastic scintillators are indicated in what follows with progressive numbers starting from the machine vacuum chamber, which is represented in a transversal section at the center of fig. 2. (Counters above and below the vacuum chamber, as well as the part of the telescopes beyond counter 6, and the flash-tube chambers are of no relevance for the analysis of the events discussed in this paper). The first thin foil kinematical chamber gives the trajectories of the particles with an overall accuracy of ± 1 mm and ± 15 mrad. The succeding thick plate spark chambers identify the electrons by the showers and determine the muon range.

§ 3. – Electronic trigger and calibrations

A simplified block diagram of the fast logic circuitry is shown in fig. 3. The final pulse which triggers the optical chambers and the film advance mechanism is defined by I E $(T_1 + T_r)$, that is the coincidence between the signals from the two wide angle telescopes and from at least one of the tagging counters. The tagging signal is defined for the left and the right tagging counters respectively as $T_1 = T_{11}\, T_{12}\, \bar{S}_1\, RF$ and $T_r = T_{r1}\, T_{r2}\, \bar{S}_r\, RF$ where $T_{11}\, T_{12}$ or $T_{r1}\, T_{r2}$ represent the coincidence between the two photomultipliers of each counter, and RF is the phase signal of the machine radiofrequency. The counters S, in anticoincidence, reject the background due to the real bremmsstrahlung. The timing to the machine RF signal is set, in order to select only the particles in time with the beam-beam collision. The wide angle signals (I , E) are threefold coincidence among the scintillation counters S_1 , S_2 , S_3 (fig. 2) of the corresponding telescope and imply a minimum penetration of 21 gcm^{-2} for particles travelling perpendicularly to the direction of the beams.

The calibration of the tagging system was performed frequently during the runs utilizing the real bremmsstrahlung (beam-beam and beam-gas), by requiring the signal from the photon detector S to be in coincidence with the tagging counter. The negligible angular spread [14] of the real bremmsstrahlung provides a calibration method almost free from the effect of the electron angular spread.

The relation between the electron impact point given by the time difference (Δt) and the equivalent photon energy (k) is obtained by correlating Δt and the photon energy of the real bremsstrahlung (E_γ) measured by the shower counter, and simply replacing E_γ by k. The electron momentum is also simply deduced by $P = E - E_\gamma$.

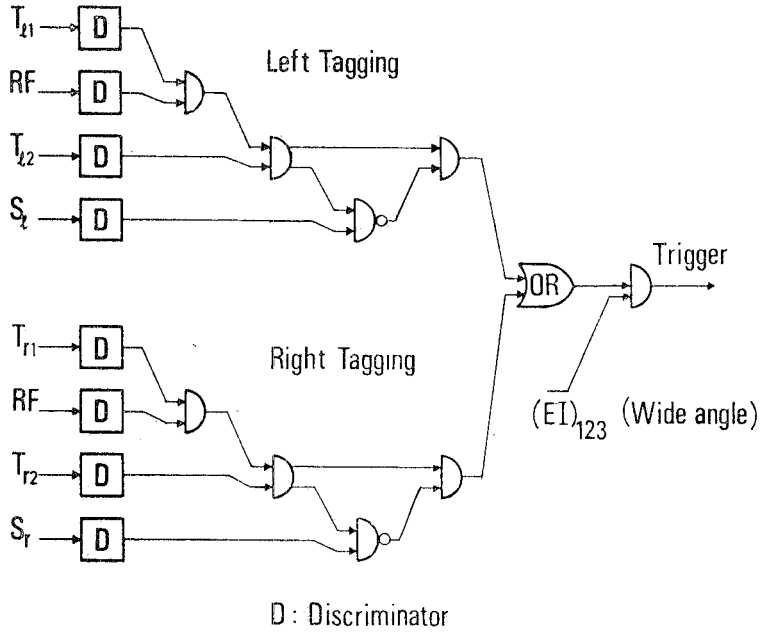

Fig. 3. – Block Diagram.

The intrinsic efficiency of each tagging counter in detecting e^+ and e^- is obtained by comparing the two energy spectra of the shower counter, *taken simultaneously*, one gated by S (RF) and the other by $T_1 T_2 \cdot S$ (RF). In this way, we can measure the efficiency as a function of x (or P, the electron momentum) within the x resolution of the shower counter. The result is consistent with an intrinsic efficiency of 95% for $0.1 \leq x \leq 0.8$. This is further confirmed by the counting rate of the double bremmsstrahlung which is selected by the coincidence:

$$((T_1 T_2)_l S_l) \quad ((T_1 T_2)_r S_r) .$$

§ 4. ANALYSIS OF THE EVENTS

The data presented here refer to energies of 800 MeV and 850 MeV per beam. The integrated luminosity is $L = 6.1 \times 10^{34}\ cm^{-2}$.

4.1. *Scanning criteria.*

For each trigger, the photograph of the wide angle telescopes are taken, together with the tagging information. The scanning criteria are as follows.

a) The kinematical spark chambers have to contain at least two tracks which converge to the source; *b*) The thick plate chambers of at least one side must show either a shower or a track with range more than 29 gcm^{-2}, which corresponds to the half of the first thick plate chamber.

Condition *a*) rejects pictures which contain no track, or single track, or tracks not converging at all. They are associated accidental triggers or " spurious " triggers due to showers produced by the stray beams hitting the vacuum chamber walls. Condition *b*) further reduces the background due to beam gas interactions.

After applying the selection criteria outlined above the remaining events are classified either into shower-shower or track-track events. No shower-track event is observed.

The events are further checked with the kinematical constraints using the tagging information.

4.2. *Kinematical constraint for* $\mu^+\mu^-$ *or* $\pi^+\pi^-$ *pair.*

For the track-track events the range of the particle can be measured with a typical accuracy of $\pm 4\%$. The kinematical relationships for $\mu^+\mu^-$ (or $\pi^+\pi^-$) are:

$$(1)\qquad \begin{aligned} \vec{k}_r + \vec{k}_1 &= \vec{P}_1 + \vec{P}_2 \quad \text{(momentum conservation)} \\ k_r + k_1 &= E_1 + E_2 \quad \text{(energy conservation)} \end{aligned}$$

where k_r and k_1 are the equivalent photon momenta, at least one of which is tagged, and $\vec{P}_1, E_1, \vec{P}_2, E_2$ are the momenta and energies of the final particles, calculated from the ranges, assuming the mass.

Assuming that the momentum lies in the beam direction [2] we have one constraint for the singly tagged events and two constraints for the doubly tagged events. The values of k_1 and k_r derived from $\vec{P}_1, E_1, \vec{P}_2$ and E_2, which are deduced from the ranges, have been compared with the ones measured by the tagging counters.

First assuming the muon mass, we get seven events in which the calculated k agrees with the measured one within the standard deviation $\pm 10\%$ (maximum observed deviation 14%). These seven events show small non-coplanarity (maximum observed $\Delta\varphi$ is 10^0), strong non-collinearity and good transverse momentum balance, which are characteristic of two body photon-photon reactions.

If the pion mass instead of the muon mass is introduced in analyzing these seven events, the reconstructed equivalent photon energy k differs from the

(2) The tagged equivalent photons have an average transverse momentum of about 2 MeV/c.

tagged one by + 20% on the average. Furthermore because none of the events exhibit nuclear interaction for combined total path length of 700 gcm^{-2}, we can conclude that these events are actually from the process $\gamma\gamma \to \mu^+ \mu^-$.

We have observed one additional event showing nuclear absorption in one of the telescopes. Measuring the range on the other telescope and assuming transverse momentum balance, this event satisfies the kinematical constraint for $\gamma\gamma \to \pi^+ \pi^-$. We consider this event as a candidate for $e^+ e^- \to$ $\to e^+ e^- \pi^+ \pi^-$.

In addition we also have seen three singly tagged events which do not fit kinematics for $\gamma\gamma \to \mu^+ \mu^-$ nor $\gamma\gamma \to \pi^+ \pi^-$ (reconstructed k differs from measured one by more than 40%). As to be explained in sec. 44, these events are probably due to beam-gas interactions, and we do not consider them as candidates for the photon-photon interaction.

4.3. *Analysis of the shower–shower events.*

For the shower-shower events, the energy of the final particles cannot be measured accurately enough. Since all these events show small non-coplanarity ($\Delta\varphi < 10^0$), the equations (1) can well be approximated by:

$$\beta = \frac{k_r - k_1}{k_r + k_1} = \frac{\sin(\theta_1 + \theta_2)}{\sin\theta_1 + \sin\theta_2}$$

where β is the velocity of the $\gamma\gamma$ system in the laboratory system, θ_1 and θ_2 are the angles of the wide angle electrons with respect to the beam direction. For doubly tagged events this gives one constraint. For singly tagged events we can calculate the unknown value of $k_r\,(k_1)$ using the measured θ_1, θ_2 and $k_1\,(k_r)$, and check for the inequality $0 \leq k_r\,(k_1) \leq E$. Thirteen events have passed through this cut and are considered the events $\gamma\gamma \to e^+ e^-$.

Two events failed, giving reconstructed $k_r\,(k_1)$ larger than the incident beam energy. This would imply that the two forward electrons are emitted in the same side and cannot be understood in the equivalent photon approximation. These events would be rather explained [9] [15] as the process $e^+ e^- \to e^+ e^- e^+ e^-$ in which the wide angle apparatus detects a primary electron that has been scattered by one of the electrons produced in the photon-photon collision. We will not further investigate, in this paper about this kind of event.

4.4. *Background.*

Beam-gas interaction could give a small angle electron on to the tagging counter and particles at wide angle telescope simulating the tagging photon-photon events. This kind of background has been measured in special runs with two separated beams. We have observed one singly tagged event during separated beam runs which in total corresponds to 20% of the total integrated luminosity of the colliding beam runs. This single event does not satisfy the

kinematics for $e^+ e^- \to e^+ e^- \mu^+ \mu^-$ nor $e^+ e^- \to e^+ e^- \pi^+ \pi^-$ with apparent unbalance of transverse momentum indicating that the three " poor fitting " events of the same nature which are observed during the colliding beam runs are mainly due to the beam gas interaction. We stress that no " good " event is observed during the separated beam runs.

The rate of accidental coincidences between the wide angle telescopes and the tagging counters was measured by using the collinear Bhabha-scattering events. No tagged event has been found out of 4000 Bhabha-scattering events, in agreement with the accidental rate 4×10^{-4} (for each wide angle trigger) expected from the combined single rate of the tagging counters (of 4×10^3/sec [3]).

5. Results

The numbers of observed good events are summarized in Table I, fig. 4 shows the scatter plot of the events in k_1 , k_r plane, where k_1 and k_r are the equivalent photon energies measured and/or reconstructed. The k_1 , k_r plane has been divided into three regions: A , B , C. The region A is accessible only

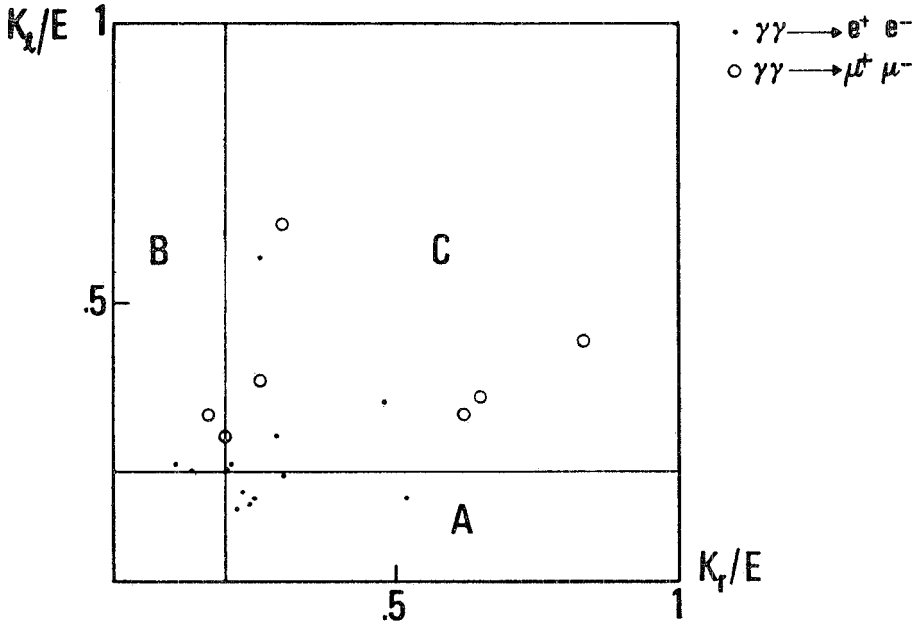

Fig. 4. – Scatter plot of the observed events.

(3) The number of bunches passing an intersection is 9×10^6/sec.

A typical working condition of ADONE around 800 MeV are average luminosity 10^{32} cm^{-2} hr^{-1}, currents 20 mA × 20 mA, mean life time 10 hours, and vacuum around intersection 10^{-9} mmHg.

to T_r events, region B to T_1, the region C to both T_r and T_1. In Table I we present also the expected numbers of events calculated as follows:

1) The *equivalent photon approximation* is used in calculating the cross section. The accuracy of the approximation is believed to be better than 10% under the kinematical conditions of this experiment.

TABLE I

		Singly tagged	Doubly tagged	Sum
$e^+ e^- \to e^+ e^- e^+ e^-$	Calculated . . .	10.9	1.9	12.8
	Observed . . .	10	3	13
$e^+ e^- \to e^+ e^- \mu^+ \mu^-$	Calculated . . .	8.0	2.9	10.9
	Observed . . .	6	1	7

2) The angular spread of the forward going $e^\pm$ is taken into account in calculating the tagging efficiency. For this purpose a Monte-Carlo program generated the $e^\pm$ according to the angular distribution based on the equivalent photon approximation [2]. The trajectory of each e^+ is followed through the quadrupoles and the bending magnets to see if it hits or misses the tagging counter. The calculated efficiency curve is shown in fig. 5.

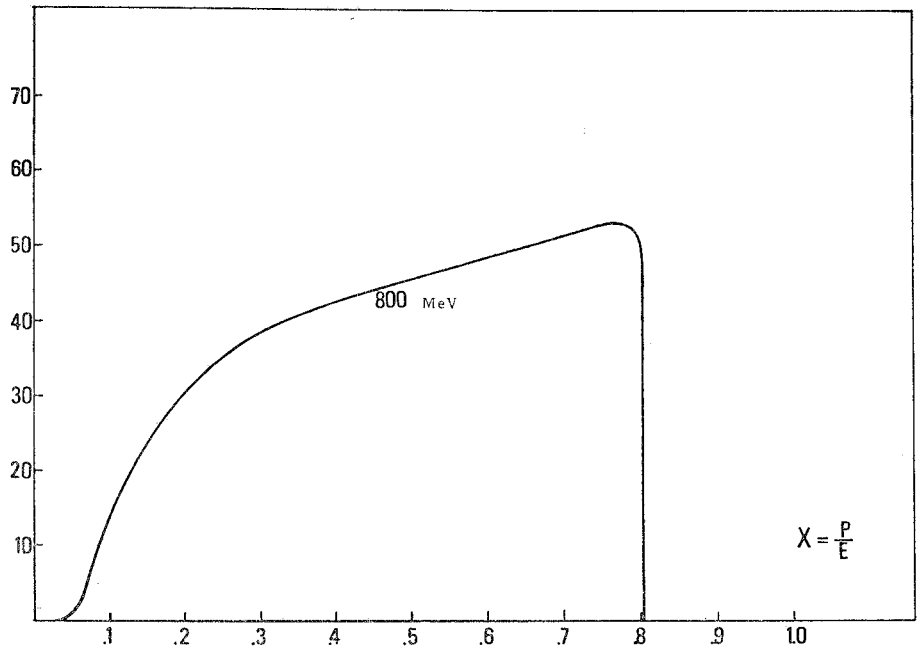

Fig. 5. – Angular efficiency of the tagging counters.

The average tagging efficiency $\bar{\varepsilon}$ can be obtained also experimentally from the ratio $\bar{r}$ between the doubly and singly tagged events inside the region C of fig. 4, since $\bar{r}$ and $\bar{\varepsilon}$ are related by:

$$\bar{r} = \frac{2\bar{\varepsilon} - \bar{\varepsilon}^2}{\bar{\varepsilon}^2} .$$

The observed value of $\bar{r}$ is 3 ± 1.7. This yields $\bar{\varepsilon} = 0.50 \pm 0.28$ in agreement, within the large statistical error, with the value of $\bar{\varepsilon}$ calculated by the Monte Carlo program.

3) The gaussian distribution of the $e^+ e^-$ interaction points along the beam direction is taken into account. This distribution is determined experimentally from the analysis of the collinear Bhabha-scattering events [10].

4) For the efficiency of the wide angle telescopes in detecting the electrons or positrons, we used the experimental values measured [16] by sending the electron beams of known energies from Frascati Synchrotron to the actual telescopes.

This equivalent photon calculation predicts 12.8 events for $e^+ e^- \to \to e^+ e^- e^+ e^-$ and 10.9 events for $e^+ e^- \to e^+ e^- \mu^+ \mu^-$ which are in good agreement with the observed 13 events of $e^+ e^- \to e^+ e^- e^+ e^-$ and 7 events of $e^+ e^- \to e^+ e^- \mu^+ \mu^-$ within the statistical errors of $\pm 30\%$.

§ 6. Contamination to the hadronic annihilation process

In the previous papers [16] [17] on e^+e^- annihilation into hadronic final states, possible contaminations from the photon-photon interaction was not investigated experimentally. In order to determine this contamination, we took all the tagged events and applied to them the same procedure that was adopted in the analysis of the hadronic processes $e^+ e^- \to$ multihadrons and $e^+ e^- \to \pi^+ \pi^-$ or $k^+ k^-$.

For the multihadron channels the criteria were essentially to retain either two track events with non-complanarity larger than 10° or events with three or more tracks. Only one tagged event was found among those fulfilling these criteria. This gives $3 \pm 3\%$ for the contamination from the photon photon process to the annihilation cross section $e^+ e^- \to$ multihadrons for our specific detector at total $e^+ e^-$ energy of 1. 6 GeV.

2) For the hadron pair production, $e^+ e^- \to \pi^+ \pi^-$ or $k^+ k^-$, the requirements were the presence of two tracks collinear within 8 degrees.

Since no tagged event satisfies these requirement the upper limit for the photon-photon contamination to the $e^+ e^- \to \pi^+ \pi^-$ or $k^+ k^-$ is of 6%.

Acknowlegement. We are indebted to Prof. M. Conversi for his contribution to the present work. Sincere thanks are due to Drs. A. Bramon and M. Greco for discussions on the theoretical aspects and to Dr. H. Ogren for his reading of the present paper. We thank the machine group for the smooth running of Adone and for allowing us to use the shower counters of their monitor.

REFERENCES

[1] N. A. ROMERO, A. JACCARINI, P. KESSLER and J. PARISI; *a*) « C. R. Acad. Sci. Sez. », B296 (1969) and 1129; *b*) « Lett. Nuovo Cimento », *4*, 933 (1970); *c*) « Lett. Nuovo Cimento », *1*, 935 (1971).
[2] S. J. BRODSKY, T. KINOSHITA and H. TERAZAWA; *a*) « Phys. Rev. Lett. », *25*, 972 (1970); *b*) « Phys. Rev. », D*4*, 1532 (1971).
[3] A. BRAMON and M. GRECO, « Lett. Nuovo Cimento » *2*, 522 (1971).
[4] M. GRECO, « Nuovo Cimento », *4* A, 689 (1971).
[5] V. E. BALAKIN *et al.*, « JETP Letters », *11*, 388 (1970). V.M. Budnev and T. F. Ginsburg: Novosibirsk Report TP–f5 (1970).
[6] For other references see the Rapporteur talk by J. Brodsky at Cornell Conferences.
[7] G. BARBIELLINI and S. ORITO, LNF–71/17.
[8] V. E. BALAKYN *et al.*, « Phys. Lett. », *34* B, 663 (1971).
[9] C. BACCI *et al.*, « Lett. Nuovo Cimento », *3*, 709 (1972).
[10] B. BORGIA *et al.*, « Phys. Lett. », *35* B, 340 (1971).
[11] B. BORGIA *et al.*, « Lett. Nuovo Cimento », *3*, 115 (1972).
[12] G. VIGNOLA, LNF–71/15.
[13] H. C. DEHNE *et al.*, LNF–72/75.
[14] S. TAZZARI, LNF–67/73.
[15] This explanation was first suggested by N. Cabibbo and G. Parisi.
[16] M. GRILLI *et al.*, « Il Nuovo Cimento », *13* A, 593 (1973).
[17] G. BARBIELLINI *et al.*, « Lett. Nuovo Cimento », *6*, 557 (1973).

ROMA, 1974 — Dott. G. Bardi, Tipografo dell'Accademia Nazionale dei Lincei